Chemical Science

ROYAL SOCIETY OF CHEMISTRY

EDGE ARTICLE

View Article Online
View Journal | View Issue

Cite this: *Chem. Sci.*, 2025, **16**, 20875

All publication charges for this article have been paid for by the Royal Society of Chemistry

Detection of single-cell enzyme activity by single-time-point stable isotope probing-mass spectrometry

Xianzhe Wu,[a] Qingxi Ma,[a] Haoran Chen,[a] Chuhao Cheng,[a] Jiapu Li,[a] Feifei Xu*[a] and Yun Chen *[abcde]

Received 7th June 2025
Accepted 29th September 2025

DOI: 10.1039/d5sc04171f

rsc.li/chemical-science

Elucidation of single-cell enzyme activity is essential for clarifying cellular heterogeneity and its causal relationship with cell fate. In the currently available methods for enzyme activity detection, the traditional multiple-time-point approaches using the Michaelis–Menten model are susceptible to prolonged measurement periods and thus compromise normal cellular functions, whereas the single-time-point approaches using Lineweaver–Burk plots are limited by sample inequality and difficulty of aliquoting a single-cell sample. Mass spectrometry (MS) has the attractive advantage of simultaneous detection of multiple molecular components. Among the MS-based assays, stable isotope probing (SIP)-MS has provided an idea of single-cell enzyme activity analysis using a single-time-point approach. In this study, a single-time-point SIP-MS assay was developed for revealing enzyme activity heterogeneity in breast cancer single cells. Specifically, a series of stable isotope labelled substrate peptides were pooled to estimate the activity of target enzyme Cathepsin D (CTSD). The results indicated the cellular heterogeneity of CTSD activity and the positive correlation between CTSD activity and the metastatic capability of cells. Furthermore, the fusion of cancer cells with M2 macrophages, as a representative cellular event in cancer development, was monitored using the developed single-time-point SIP-MS assay. Owing to their greater metastatic potential, the fused cells could be well distinguished from the unfused cells based on the detected CTSD activity at the single-cell level.

Introduction

As it is well known, cancer cells are heterogeneous in gene expression, protein function, enzyme activity, metabolic phenotype and ultimately cellular function.[1] Phenotypic differences in individual cells such as cancer metastatic potential can be regarded as the macroscopic manifestations of cellular heterogeneity.[2] A good illustration of this causal relationship between cell heterogeneity and fate decision is the difference in enzyme activity, which plays a key role in cellular functions.[3] For example, the activity of Cathepsin D (CTSD) is closely related to cellular migration capability and thus cancer metastasis and progression.[4] Furthermore, there is evidence indicating the cellular heterogeneity in CTSD activity; the cells with high CTSD activity can effectively break through tissue barriers and achieve metastasis.[5]

In traditional studies, cell functions were normally evaluated by bulk cell analysis. Because bulk cell analysis normally provides average results and may overlook important features resulting from inherent heterogeneity, single-cell assays have been increasingly developed for elucidating cellular heterogeneity in recent years.[6] Among the single-cell assays, enzymatic assays are among the most attractive ones probably due to the key role of enzymes in cells, which arises from upstream gene expression, determines the downstream outcomes of metabolic pathways,[7] ultimately defines the cellular functions[8] and may also be targets for drug action.[9] To date, there are a couple of techniques available to study enzymes in single cells, most of which focus on enzyme protein expression.[10] Unfortunately, few studies were carried out for the detection of single-cell enzyme activity.[11]

The currently available studies of single-cell enzyme activity are mainly based on the techniques of imaging, microfluidics, flow-through systems, capillary electrophoretic separation, or combinations of these. Provided that enzyme activity normally depends on the enzyme–substrate interaction,[12] most of the previous studies used the amount of enzymatic product generated per unit time in multiple-time-point plots for estimating the reaction rate[13] or Michaelis constant (K_m) in the Michaelis–

[a]*School of Pharmacy, Nanjing Medical University, Nanjing, 211166, China. E-mail: ychen@njmu.edu.cn; feifeixu@njmu.edu.cn; Fax: +86-25-86868467; Tel: +86-25-86868326*

[b]*State Key Laboratory of Reproductive Medicine and Offspring Health, Nanjing, 211166, China*

[c]*Key Laboratory of Cardiovascular & Cerebrovascular Medicine, Nanjing, 211166, China*

[d]*Innovation Center of Suzhou Nanjing Medical University, Suzhou, 215000, China*

[e]*National Center of Technology Innovation for Biopharmaceuticals, Suzhou, 215000, China*

Menten equation.[14] Alternatively, the reaction rates at different substrate concentrations in equal samples at a single time point can also provide the value of K_m using Lineweaver–Burk plots (double inverse plots).[15] Notably, the multiple-time-point approach is usually selected for the study of single-cell enzyme activity due to the inequality of aliquoting a single-cell sample in the single-time-point approach and the difficulty of miniaturization of most techniques. However, long-term and repeated detection in the same cells is susceptible to the prolonged measurement periods and thus compromises normal cellular functions. Therefore, smarter single-cell enzyme assays are urgently expected in cellular heterogeneity research.

Mass spectrometry (MS) has the advantages of high selectivity and quantitative capability. More importantly, it is capable of simultaneous detection of multiple components.[16] Among the MS-based assays, stable isotope probing (SIP)-MS enables simultaneous tracing of a series of stable isotope labelled molecules with different molecular weights.[17] This assay provides an idea of applying SIP-MS for the simultaneous detection of multiple isotope labelled substrates/products in single cells using a single-time-point enzyme activity approach.

In this study, a SIP-MS assay was developed for single-cell enzyme activity detection (Fig. 1). A series of stable isotope labelled substrate peptides were loaded into single cells and detected at a single time point to estimate the single-cell activity of target enzyme CTSD. Using the developed assay, the single-cell CTSD activity in breast cancer MDA-MB-231 cells and MCF-7 cells was determined. In addition, the heterogeneity of the detected enzyme activity in single cells was also studied and was further associated with the cell metastatic capability. Furthermore, the fusion of cancer cells with M2 macrophages, as a representative cellular event in cancer metastasis, was monitored by the developed SIP-MS assay.

Results and discussion

Fulfillment of MS detection criteria for single-time-point SIP-MS assay

In this study, there are two prerequisites for the SIP-MS assay, including (a) MS detection of substrates/products in a single cell sample and (b) the ability to collect reaction rates at different substrate concentrations at a single time point

(a) MS detection in a single cell

For the first prerequisite, CTSD can catalyze the cleavage of the peptide EEISEVNLDAEFRG (*i.e.*, PEP1) as a substrate[18] and obtain the product peptide EEISEVNL (*i.e.*, PEP4) (Fig. S1). These peptides meet the general principle of peptide selection in LC-MS/MS analysis as the peptides should (a) not be found in any protein by a BLAST search, (b) provide an adequate mass response, and (c) produce high-quality multiple reaction monitoring (MRM). The most abundant form of the product peptide PEP4 in the mass spectrum was a doubly charged ion, and the MRM transitions with the highest signal-to-noise (S/N) ratios and limits of quantification (LOQs) were provided by the fragment ions b2 *m*/*z* 259.1, b5 *m*/*z* 588.4, and b6 *m*/*z* 687.4 (Fig. 2A). Furthermore, the linear detection range of PEP4 spans 10.0 pM–250 nM (Fig. S2), satisfying the submicromolar detection of enzymatic reaction products in single cells. Validation results demonstrated good accuracy and precision of the MS detection (Tables S1–S3). Therefore, PEP1 was selected as the primary substrate peptide and PEP4 as the primary product peptide in this study.

(b) MS detection at a single time point

The second prerequisite for the SIP-MS assay is that the information on the reaction rates can be collected at a single time point as described above. Because current methods involving mass spectrometry are not suitable for high-throughput analysis of multiple samples on the timeline, novel approaches are needed to differentiate and analyze all the substrate peptides and product peptides simultaneously at different substrate concentrations.[19] To realize this simultaneous detection and accurate quantitative analysis of multiple peptides, the SIP technique was employed and stable isotope labelled substrate peptides were proposed in the same sample, leveraging their distinct mass differences but nearly identical chemical and biological behavior.[12] Specifically, the MS detection of stable isotope labelled substrate/product peptides can be easily differentiated from that of nonlabelled ones, attributed to the mass shift of the isotope labelling. Thus, in addition to nonlabelled PEP1, the other two isotope labelled peptides PEP2

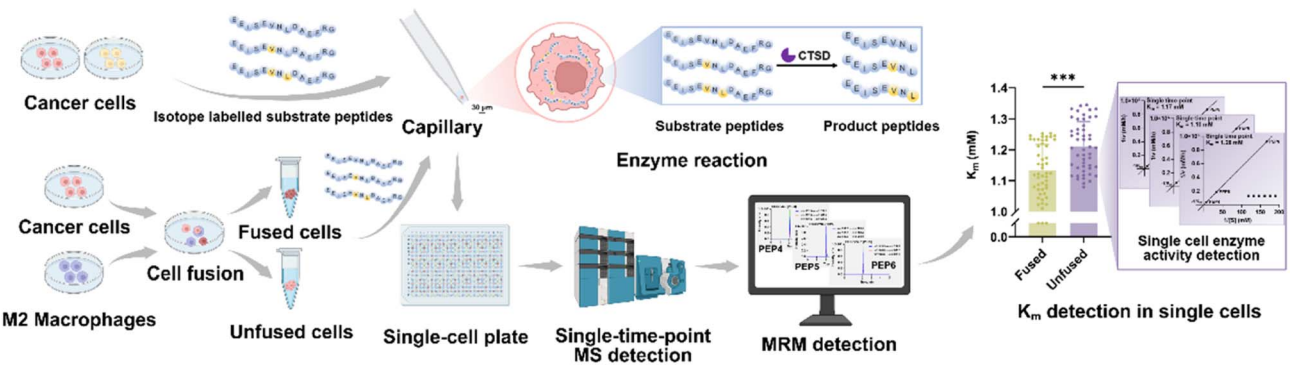

Fig. 1 Working schematic of the SIP-MS assay for single-cell enzyme activity detection. In detail, a series of stable isotope labelled substrate peptides are loaded into single cells, and the product peptides are detected at a single time point to estimate the single-cell activity (K_m) of the target enzyme using Lineweaver–Burk plots. Using the developed assay, the single-cell CTSD activity in breast cancer MDA-MB-231 cells, SK-BR-3 cells, MCF-7 cells and fused cancer cells with M2 macrophages was determined.

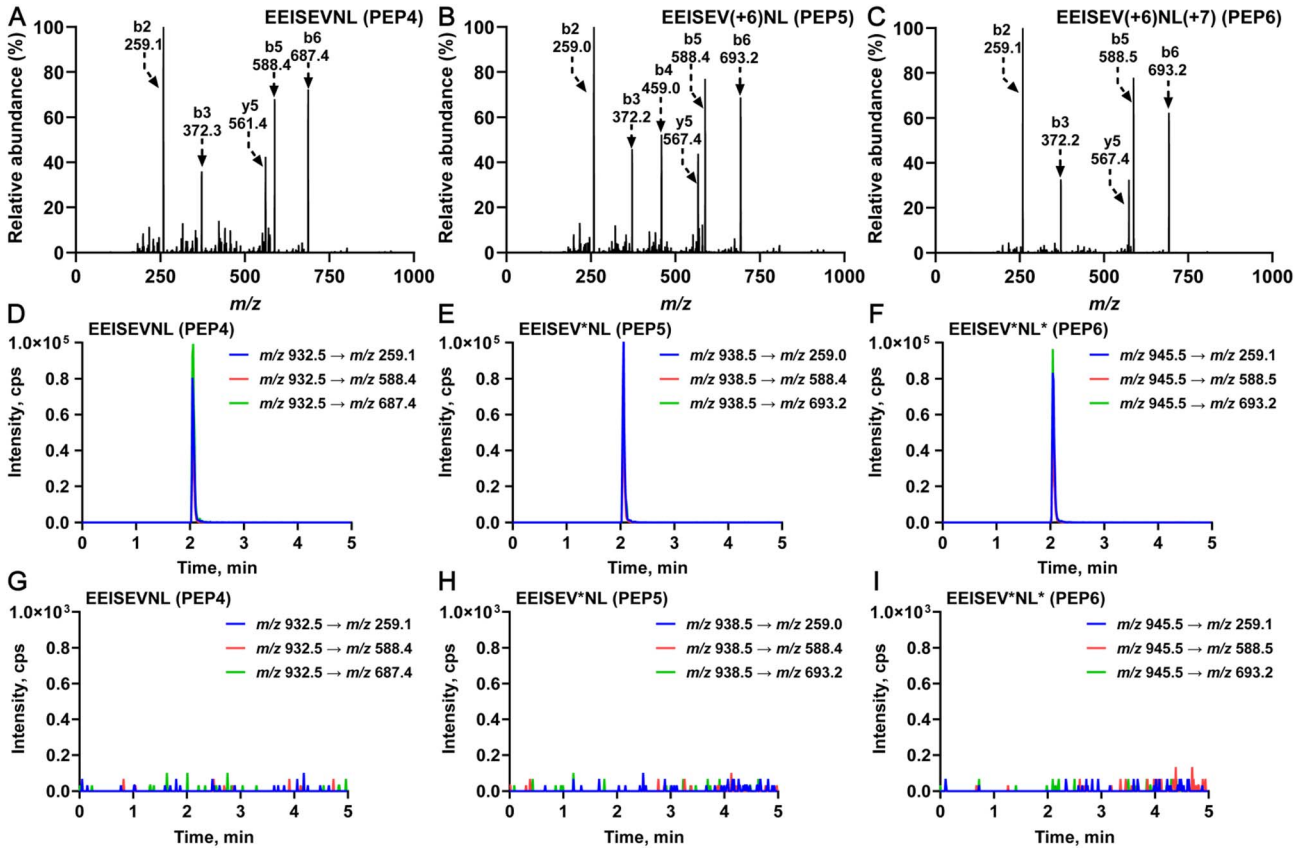

Fig. 2 (A–C) Fragment ion spectra of the product peptides PEP4, PEP5 and PEP6. (D–F) LC-MS/MS chromatograms of the product peptides. (G–I) LC-MS/MS chromatograms of mixtures of two product peptides using the MRM transitions of the third product peptide. In detail, (G) represents the detection of PEP4 in a mixed solution of PEP5 and PEP6, (H) represents the detection of PEP5 in a mixed solution of PEP4 and PEP6 and (I) represents the detection of PEP6 in a mixed solution of PEP4 and PEP5.

EEISEV*(Val-13C5,15N)NLDAEFRG with stable isotope labelling of valine (Val, V) and mass shift of 6, and PEP3 EEISEV*(Val-13C5,15N)NL*(Leu-13C6,15N)DAEFRG with stable isotope labelling of both valine and leucine (Leu, L) and mass shift of 13 were carefully selected. The corresponding peptide products for these three substrate peptides were PEP4 EEISEVNL, PEP5 EEISEV*NL, and PEP6 EEISEV*NL*. Notably, the fragment ions cleaved at the same bond were selected as the product peptides. More importantly, the isotope labelled amino acids were included in the selected product peptides to maximize the difference of MRM transitions of PEP4, PEP5 and PEP6 (Table 1). As shown in Fig. S3 and S4, some product ions of the labelled PEP2 and PEP3 have *m*/*z* differences of 6 and 13 from those of the nonlabelled PEP1, respectively. The *m*/*z* differences of the selected product ions of PEP5 and PEP6 from that of PEP4 were 6, respectively (Fig. 2B and C). In addition, SEVNL was chosen as the internal standard. The results indicated reliable MS detection of the peptides (Fig. 2D–F) and confirmed that there was no cross-talk among the MRMs of the substrates and products (Fig. 2G–I and S5), in addition to the absence of endogenous interference from cells (Fig. S6). It is worth noting that the

Table 1 MRM transitions of the substrate peptides, product peptides and internal standard (IS)

Peptide sequence	MRM transition
EEISEVNLDAEFRG (PEP1)	804.5 → 694.5
	804.5 → 921.7
	804.5 → 1020.5
EEISEV*NLDAEFRG (PEP2)	807.6 → 694.4
	807.6 → 921.5
	807.6 → 1027.6
EEISEV*NL*DAEFRG (PEP3)	811.1 → 694.5
	811.1 → 928.6
	811.1 → 1033.5
EEISEVNL (PEP4)	932.5 → 259.1
	932.5 → 588.4
	932.5 → 687.4
EEISEV*NL (PEP5)	938.5 → 259.0
	938.5 → 588.4
	938.5 → 693.2
EEISEV*NL* (PEP6)	945.5 → 259.1
	945.5 → 588.5
	945.5 → 693.2
SEVNL (IS)	561.4 → 246.2
	561.4 → 345.3
	561.4 → 430.3

peptides used in SIP-MS assays are relatively easy to prepare, less susceptible to environmental interference, and offer greater potential for multiplexing compared to the methods relying on fluorescent or electrical signals.[20,21]

Development of single-time-point SIP-MS assay for determining single-cell enzyme activity

As described earlier, the K_m value reflects the efficiency of enzyme–substrate binding and can represent enzyme activity. By studying K_m, we can better understand the function and role of enzymes in biochemical processes. In particular, analysis of K_m in single cells can provide information about variability in the individual biochemical steps that affect downstream outcomes, and these may elucidate the biochemical origins of cellular heterogeneity.[7]

After selecting substrate peptides and product peptides for single-time-point SIP-MS, another concern that deserved consideration for single-cell enzyme activity detection was satisfying the criteria for reliable Lineweaver–Burk plots. The enzyme activity detection in bulk cells usually estimated the K_m value by non-linear fitting of the Michaelis–Menten equation at multiple time points[22] or from Lineweaver–Burk plots (double inverse plots) of different substrate concentrations at single time point after equalization of the samples.[15] Different from these traditional approaches, our study innovatively modified the method of Lineweaver–Burk plots and employed multiple isotope labelled substrates in the enzyme activity detection. Several conditions must be met for the use of Lineweaver–Burk plots, such as the specificity of enzyme–substrate interaction and the total concentrations of substrates in the developed assay.[23]

In general, the ability of a specific enzyme to cleave a specific substrate is known as specificity, including both substrate specificity and enzyme specificity.[24] For enzyme specificity, it is not easy to exclude other endogenous compounds cleaved by CTSD. As previously reported, CTSD can preferentially cleave the peptides containing both leucine (Leu, L) and aspartic acid (Asp, D). The substrate peptide employed in this study is the one with the greatest reactivity reported so far, which was also validated here (Fig. S7). Moreover, when the CTSD enzyme was inhibited with pepstatin A, the level of substrate peptides remained stable and negligible product peptides were detected (Fig. 3A and S8). For the evaluation of substrate specificity, the substrate peptides were incubated with cells, and the amount of product peptides obtained declined dramatically with the addition of pepstatin A, demonstrating the absence of endogenous interference (Fig. 3B and S8). Finally, no change occurred for the product peptides in the presence of cells (Fig. 3C).

Another condition for using Lineweaver–Burk plots at a given time point is that there is no competitive inhibition between the substrates, which can be satisfied as long as the sum of the substrate concentrations is much smaller than the K_m value (total substrate concentration/K_m < 0.2).[25] Under such circumstances, the system operates in the first-order kinetic regime for each substrate peptide, where the enzyme is far below saturation and the reaction velocity depends linearly on the substrate concentration. Using the multiple-time-point MS approach and Michaelis–Menten equation, a K_m value of 1.12 ± 0.02 mM was first obtained for the CTSD enzyme (Fig. 4A), which was consistent with that previously reported in the public database.[18] In addition, there was no difference in the calculated values of K_m by varying the CTSD concentration (1.00–50.0 nM) ($p > 0.05$) (Fig. 4A).[26] Furthermore, the CTSD enzyme activity in cells was also evaluated and the obtained K_m value of 1.15 ± 0.08 mM was close to that using CTSD enzyme alone (Fig. 4B), further confirming the negligible interference from cells. The obtained K_m value using the single-time-point MS approach in bulk cell analysis was 1.18 ± 0.02 mM, which was not significantly different from the one estimated by the Michaelis–Menten equation using multiple time points (1.15 ± 0.08 mM) (Fig. 4C).

Regarding the determined K_m value, the concentrations of PEP1, PEP2, and PEP3 were set as 150 μM, 30.0 μM, and 6.00 μM, and the total substrate concentration/K_m was controlled at <0.03. The results further indicated that the MS signal of the product peptides in the multiple-substrate reaction was the same as that in the single-substrate reaction, confirming that there was no competitive inhibition between the substrate peptides in this system (Fig. 4D).

Finally, single cells were sorted into 384-well plates by flow cytometry and detected by the single-time-point SIP-MS assay (Fig. S9). During this process, technical variability due to factors

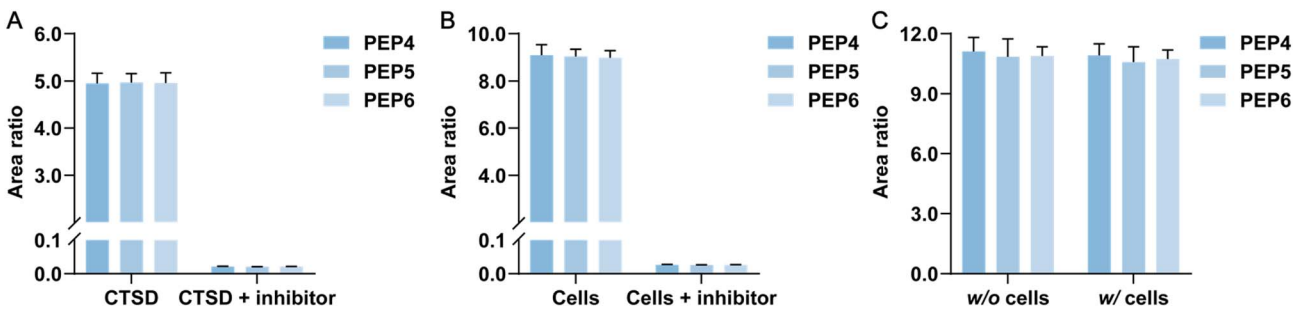

Fig. 3 (A) MS signals of the product peptides after the incubation of the substrate peptides and CTSD enzyme for 4 h with and without the treatment of a CTSD inhibitor pepstatin A. (B) MS signals of the product peptides after the incubation of the substrate peptides and MCF-7 cell lysate for 4 h with and without the treatment of pepstatin A. (C) MS signals of the product peptides after their incubation with and without MCF-7 cell lysate for 4 h. Specifically, 50 μL of reaction buffer containing 300 nM internal standard and 200 nM substrate peptide (*i.e.*, PEP1, PEP2 and PEP3) was mixed with 10 μL of 180 nM CTSD enzyme or cell lysate to generate product peptides (*i.e.*, PEP4, PEP5 and PEP6).

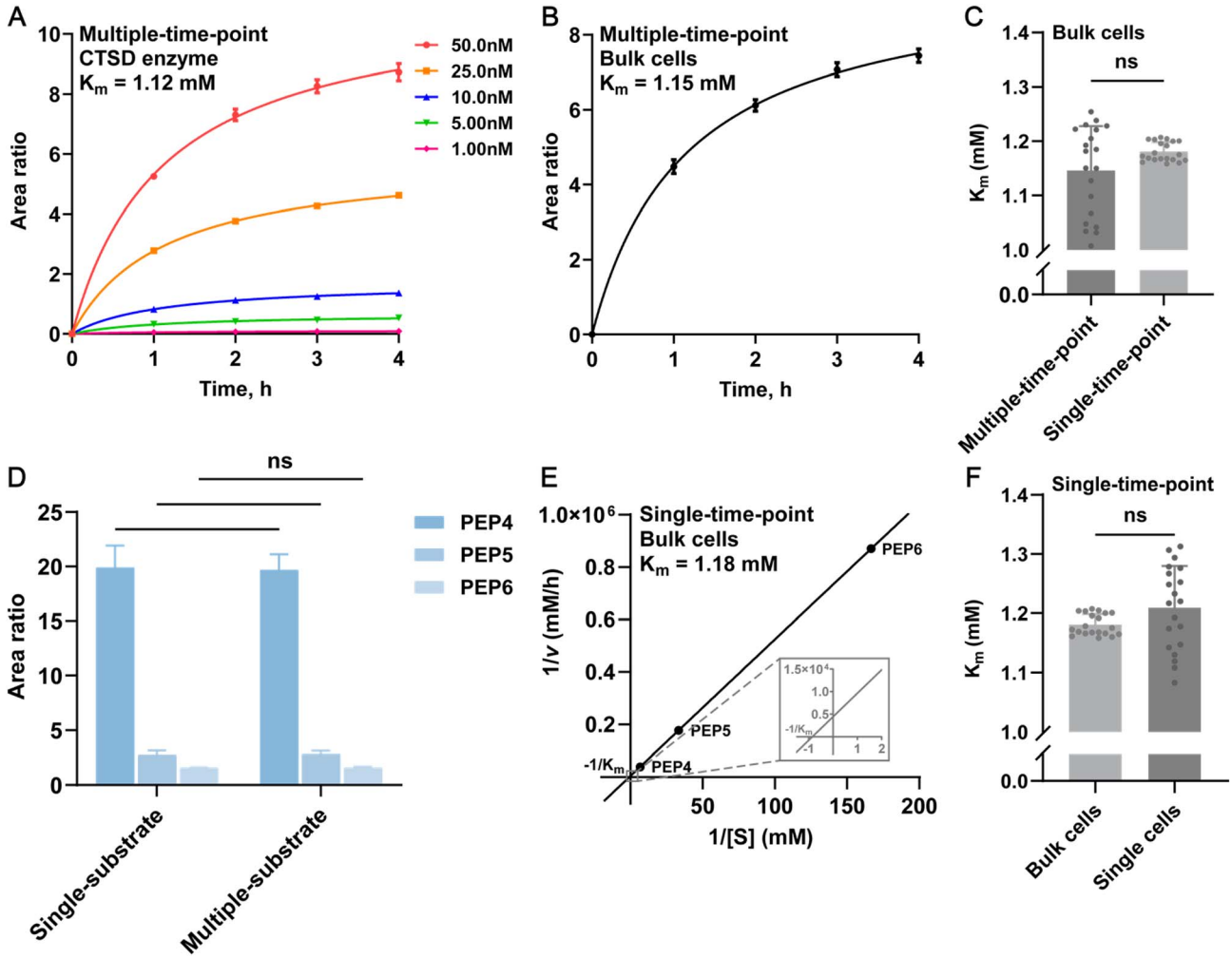

Fig. 4 (A) Multiple-time-point MS approach and Michaelis–Menten analysis of the CTSD enzyme activity by detecting PEP4 at different enzyme concentrations. 150 μM PEP1 was mixed with five CTSD samples, respectively, and the reaction was carried out for 0 h, 1 h, 2 h, 3 h and 4 h. The obtained K_m values at the CTSD concentrations of 1.00 nM, 5.00 nM, 10.0 nM, 25.0 nM, and 50.0 nM were 1.17 mM, 1.13 mM, 1.11 mM, 1.14 mM, and 1.12 mM, respectively. (B) Multiple-time-point MS approach and representative Michaelis–Menten analysis of the CTSD enzyme activity in MCF-7 cell lysate. (C) Comparison of the K_m values of CTSD determined by the multiple-time-point MS and single-time-point MS approaches in MCF-7 cell lysate. ns: not significant. (D) MS signals of the product peptides after incubating the CTSD enzyme with individual substrate peptides and mixed substrate peptides at the same concentrations, respectively. (E) Representative detection of K_m in MCF-7 cell lysate using Lineweaver–Burk plots and by detecting PEP4, PEP5 and PEP6 at a single time point. For the SIP-MS assay, 50 μL of reaction buffer containing 180 μM PEP1, 36.0 μM PEP2, 7.20 μM PEP3 and 300 nM internal standard with 0.5% Triton X-100 was mixed with 10 μL of cell lysate for 4 h. (F) Single-time-point SIP-MS assay for the detection of K_m in MCF-7 cell lysate and single cells. Notably, the CTSD enzyme concentration in cells was estimated to be ~0.08 μM in advance, according to the previous studies. ns: not significant.

such as permeabilization time and experimental temperature was strictly controlled for minimal perturbations to the cellular microenvironment. As a result, the K_m value can be well determined for individual cells (Fig. 4E).[27] The mean of the K_m value of CTSD in single cells was calculated to be 1.20 ± 0.08 mM, close to that determined in bulk cells (Fig. 4F).

Detection of heterogeneity in the CTSD enzyme activity of breast cancer single cells

The established single-time-point SIP-MS assay was then used to estimate the K_m value of CTSD in MCF-7 (Luminal), SK-BR-3 (HER2+) and MDA-MB-231 (TN) single cells (Fig. 5A). First, the mean K_m values of CTSD in MDA-MB-231 cells (1.14 ± 0.06 mM) and SK-BR-3 cells (1.15 ± 0.06 mM) were not different from each other, but significantly lower than that of MCF-7 cells (1.19 ± 0.07 mM) (Fig. 5B), demonstrating a potential positive relationship between CTSD activity and metastatic capability of cells. Previous studies have also shown that CTSD is closely related to the metastatic capability of breast cancer. Although CTSD is predominantly located and active in acidic organelles, evidence has indicated that CTSD can be secreted into the cytoplasm or nucleus as well as the extracellular milieu (ECM), thus playing an important role in protein degradation both inside and outside the cells.[4] As a result, ECM components can be broken down, facilitating tumor cell invasion. Moreover, CTSD can activate other proteases such as matrix metalloproteinases (MMPs) that can further break down tissue

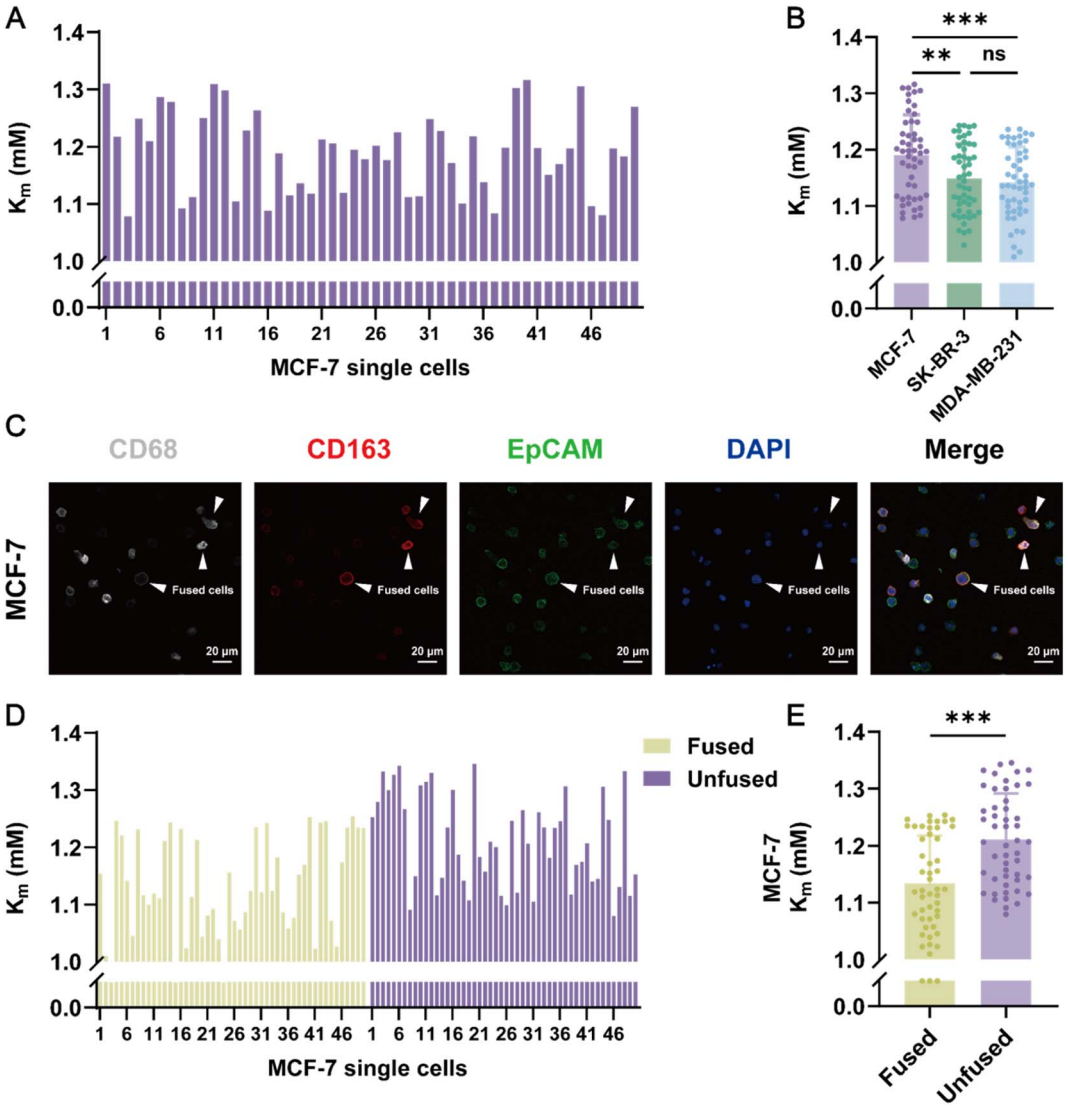

Fig. 5 (A) K_m values of CTSD in MCF-7 single cells. (B) K_m values of CTSD in MCF-7, SK-BR-3 and MDA-MB-231 single cells detected by the single-time-point SIP-MS assay. $n = 50$; $^{**}p < 0.01$; $^{***}p < 0.001$; ns, not significant. (C) Confocal microscopy images of fused and unfused MCF-7 cells. Cells were stained by immunofluorescence staining, and fused cells were defined as EpCAM$^+$ (green), CD163$^+$ (red) and DAPI$^+$ (blue). CD68 was used as a pan-macrophage marker (white). (D and E) K_m values of CTSD in fused and unfused MCF-7 single cells detected by the single-time-point SIP-MS assay $^{***}p < 0.001$.

barriers.[28] More importantly, the local microenvironment change may have a significant impact on the CTSD activity. Several studies have shown that the reduction of CTSD activity is a significant predictor of prognosis in breast cancer patients.[29]

Second, the variance of K_m in single cells was significantly larger than that of bulk cell measurements, reflecting the cell heterogeneity in CTSD activity (Fig. 4E).[30] In addition, the variance of K_m decreased as the number of detected single cells increased, approaching that of bulk cell measurements (Fig. S10). The observed heterogeneity may arise from metabolic state, ionic strength, and enzyme stability, which may be related to the cell phase, gene mutations, intracellular microenvironment, and structural changes in the enzyme.[7] Even though clinical samples were not systematically examined in this study, larger heterogeneity in CTSD activity is highly expected in these samples because MDA-MB-231 and MCF-7 cells can be considered as genetically identical cells and enzyme activity in cultured single cells should be susceptible to less factors compared to that in clinical samples.[31]

Tracking of CTSD activity in cell fusion

In general, cellular characteristics and functions are often altered together with phenotypic changes. However, single cells may exhibit differential responses during these processes. Some may resist such changes, while others may undergo more advanced transformations and play a primary role in driving phenotypic progression.[32] Therefore, single-cell CTSD activity was monitored in a cellular event, in addition to the analysis of the CTSD activity in breast cancer single cells. To date, a couple of processes including fusion between cancer cells and macrophages,

epithelial-mesenchymal transition (EMT) and stem cell conversion have been suggested as the key mechanisms driving cancer progression and metastasis.[33] Among these processes, cancer cells demonstrate a significant increase in the metastatic capability after fusion with M2 macrophages in early cancer development.[34] Therefore, identification of the fused cells and estimation of their invasion and metastasis potential are some of the challenges for prognostic assessment of cancer. In the previous studies, fused cells could only be identified by size or fluorescent antibody staining (Fig. 5C).[35] Regarding the association of CTSD activity with metastatic capability of cancer cells, the CTSD enzyme activity was monitored in the cells, which were stained and sorted by flow cytometry after fusion with the validated M2 macrophages (Fig. S11 and S12). The K_m value of CTSD in the fused MCF-7 cells with M2 macrophages was 1.13 $\pm$ 0.08 mM, which was significantly lower than that of unfused MCF-7 cells (1.21 $\pm$ 0.08 mM, $p < 0.001$) (Fig. 5D and E). In addition, the transwell experiments indicated that cell metastasis was enhanced in those fused cells (Fig. S13), confirming the positive correlation between CTSD activity and metastatic potential. These findings can also be observed in unfused and fused MDA-MB-231 cells (Fig. S14).

Further investigation was conducted in unsorted MCF-7 cells after fusion with M2 macrophages. The results indicated that there were at least two subgroups in these cells. A CTSD reference interval was calculated as 1.05 (95% CI, 1.02–1.09) mM to 1.369 (95% CI, 1.34–1.40) mM using MedCalc® software (version 20.100; MedCalc Software Ltd, Ostend, Belgium) and the data of the unfused MCF-7 cells. Thus, 4 of 50 cells after fusion have the CTSD results lower than this estimated reference interval. Their mean value was 1.03 $\pm$ 0.01 mM, which was significantly different from that of the unfused cells at a 95% confidence level and lower than that of the fused cells, probably due to the tight reference interval (Fig. 5E and S15). Interestingly, the number of cells screened based on CTSD activity was slightly higher than that analyzed by flow cytometry. This deviation was probably due to the limited number of enzymes involved in the cell identification. With the addition of more enzyme activity markers in future analysis, the performance of fused cell identification could be enhanced. Overall, the developed single-cell enzyme activity detection may benefit the finding of fused cells and thus the prediction of metastatic potential in cancer prognosis.

Conclusions

In this work, we successfully designed and developed a single-time-point SIP-MS assay for single-cell enzyme activity detection. The assay achieved the detection of CTSD activity in each single cell through the simultaneous monitoring of multiple isotope labelled substrate peptides at a single time point using MS. Theoretically, SIP-MS is a technique capable of covering a wide spectrum of stable isotopes and thus the involvement of more substrate peptides with different isotope labelling for the enzyme may achieve greater accuracy and robustness in the activity estimation. In addition, groups of substrate peptides for various enzymes can also be employed in analysis as long as the number of MRM transitions in mass spectrometry is not saturated, where more efforts will be taken to optimize reaction time, carry out substrate derivatization, adjust MS parameters, *etc.* for multiplexed detection.[36] Moreover, enhanced single-cell sorting techniques, such as those employing highly scalable microfluidic platforms (*e.g.*, microwell arrays), have the potential to significantly increase assay throughput. By integrating enzyme activity data with other single-cell omics data, the recognition of the actual state of cells and the regulatory mechanisms of key functions can be enhanced. Thus, the heterogeneous characteristics in single cells can be predicted in a more accurate manner. This information may ultimately facilitate the establishment of disease assessment models in the future.

Experimental section

Cell culture

Three human breast cancer cell lines, MCF-7 (Luminal), SK-BR-3 (HER2+) and MDA-MB-231 (triple-negative/TN), and one human monocyte leukemia cell line, THP-1, were obtained from the Cell Resource Center of the Chinese Academy of Medical Sciences (Shanghai, China). MCF-7 cells and THP-1 cells were cultured in Dulbecco's Modified Eagle Medium (DMEM) with 10% FBS and 1% penicillin/streptomycin at 37 °C with 5% CO_2. SK-BR-3 cells were cultured in McCoy's 5A with 10% FBS and 1% penicillin/streptomycin at 37 °C with 5% CO_2. MDA-MB-231 cells were cultured in RPMI 1640 containing 10% FBS and 1% penicillin/streptomycin at 37 °C with 5% CO_2. The medium was changed every 2 days and the cells were passaged every 5–7 days using 0.25% trypsin.

Construction of the fusion cell model

To generate M2 macrophages, THP-1 cells were treated with 10 ng mL^{-1} PMA for 24 h, and then cultured with 25 ng mL^{-1} IL4 and 25 ng mL^{-1} IL13 for another 48 h. Then, 5×10^6 MCF-7 cells were mixed thoroughly with an equal number of M2 macrophages and centrifuged at 800 rpm for 5 min, and the supernatant was discarded. 500 μL of 50% PEG 1450 solution was added to the cell pellet drop by drop at 37 °C, while shaking gently to disperse the cells evenly. The reaction was terminated by adding 9 mL of DMEM and centrifuged at 800 rpm for 5 min. The cell pellet was transferred to DMEM supplemented with 10% FBS and incubated for 24 h. After fusion, the cells were washed and resuspended in PBS at a concentration of 1×10^6 cells/100 μL. PE-CD163 and FITC-EpCAM were added to the cell suspension at a 1 : 50 dilution and incubated at room temperature in the dark for 2 h. Cell sorting was carried out using a BD FACS Aria II SORP high-speed flow cytometer (BD Biosciences, Franklin Lakes, NJ, USA), and the fused cells with both CD163 and FITC-EpCAM staining were collected. The cell fusion efficiency was ~6%, which agreed with the previous reports.[37]

CTSD activity detection in bulk cells using multiple-time-point MS and single-time-point MS

For the detection of CTSD activity, 150 μM substrate peptide (*i.e.*, non-labelled substrate peptide EEISEVNLDAEFRG, PEP1),

250 nM internal standard and 10.0 nM CTSD enzyme were mixed in sodium acetate buffer, and the reaction was carried out at 37 °C in a shaker.

For the multiple-time-point MS detection of CTSD activity in MDA-MB-231 or MCF-7 cells, 1×10^6 cells were washed with ice-cold PBS and resuspended in 200 μL of chilled RIPA lysis buffer. The cells were homogenized quickly and then incubated on ice for 10 min. The sample was centrifuged for 5 min at 4 °C at 3000×*g*. Afterward, 50 μL of reaction buffer containing 300 nM internal standard and 180 μM substrate peptide was added to 10 μL of cell lysate. The reaction was carried out at 37 °C in a shaker. The product peptide was detected at 0 h, 1 h, 2 h, 3 h and 4 h. The enzyme reaction rates were calculated at each time point, and K_m value was obtained by nonlinear fitting of the Michaelis–Menten equation using GraphPad Prism version 6.02.

For the single-time-point MS detection of CTSD activity in cells, 50 μL of reaction buffer containing the substrate peptide at different concentrations and 300 nM internal standard was mixed with 10 μL of cell lysate for the same time period. The reaction rate was estimated for each sample, and the K_m value was calculated using Lineweaver–Burk plots.

The calculations are described in the SI.

CTSD activity detection in single cells using single-time-point SIP-MS

Each cell in the plate was aspirated using a capillary loaded with 10 nL sodium acetate buffer containing the substrate peptides (*i.e.*, non-labelled substrate peptide PEP1, single-isotope-labelled substrate peptides (EEISEV*NLDAEFRG, PEP2 and double-isotope-labelled peptide EEISEV*NL*DAEFRG, PEP3)) at different concentrations and 0.5% Triton X-100 at the tip. The enzyme reaction was carried out for 30 min, a duration significantly shorter than that required for bulk cells. This acceleration is likely attributable to the use of capillaries with volume in the nanoliter range, which could significantly enhance reaction efficiency.[38] The method of capillary preparation is described in the SI. Afterward, 5 μL of internal standard solution containing 0.1% formic acid was added to each well of a 384-well plate, and the solution at the capillary tip was added into the 384-well plate after reaction. The sample in each well was fully mixed and analyzed directly by liquid chromatography-tandem mass spectrometry (LC-MS/MS). Using the detected concentrations of the corresponding product peptides EEISEVNL (PEP4), EEISEV*NL (PEP5), EEISEV*NL* (PEP6), the reaction rate corresponding to each substrate peptide can be estimated, and the K_m value was calculated using the reaction rates from Lineweaver–Burk plots.

Author contributions

X. W. designed and performed experiments, analyzed data, created the figures and wrote the manuscript. Q. M. performed experiments and analyzed data. H. C., C. C. and J. L. performed experiments. Y. C. and F. X. conceived the idea, supervised the study, and co-wrote the manuscript.

Conflicts of interest

There are no conflicts to declare.

Data availability

All the data supporting this article have been included in the main text and the supporting information (SI). Supplementary information: supplementary figures (S1–S15), supplementary tables (S1–S3) and supplementary materials (S1–S9) are provided. See DOI: **https://doi.org/10.1039/d5sc04171f**.

Acknowledgements

This work was supported by the National Natural Science Foundation of China (22374080, 22174068, and 21722504), Primary Research & Development Plan of Jiangsu Province (BK20221303 and BE2022796), Open Foundation of State Key Laboratory of Reproductive Medicine (SKLRM-2022BP1 and JX116GSP20240507), and Science and Technology Development Fund of NJMU (NJMUQY2022003) awarded to Dr Chen, which is gratefully acknowledged. We thank Dr Qigang Zhou and Dr Rongfeng Li from Nanjing Medical University for P-1000 capillary puller and MF2 microforge support. Some graphical elements in the abstract figure were created with **https://www.biorender.com/**.

Notes and references

1 N. Vasan, J. Baselga and D. M. Hyman, *Nature*, 2019, **575**, 299–309.
2 H. J. Woo, S. H. Kim, H. J. Kang, S. H. Lee, S. J. Lee, J. M. Kim, O. Gurel, S. Y. Kim, H. R. Roh, J. Lee, Y. Park, H. Y. Shin, Y. I. Shin, S. M. Lee, S. Y. Oh, Y. Z. Kim, J. I. Chae, S. Lee, M. H. Hong, B. C. Cho, E. S. Lee, K. Pantel, H. R. Kim and M. S. Kim, *Theranostics*, 2022, **12**, 3676–3689.
3 L. Knopfova, P. Benes, L. Pekarcikova, M. Hermanova, M. Masarik, Z. Pernicova, K. Soucek and J. Smarda, *Mol. Cancer*, 2012, **11**, 15.
4 S. Ketterer, J. Mitschke, A. Ketscher, M. Schlimpert, W. Reichardt, N. Baeuerle, M. E. Hess, P. Metzger, M. Boerries, C. Peters, B. Kammerer, T. Brummer, F. Steinberg and T. Reinheckel, *Nat. Commun.*, 2020, **11**, 5133.
5 S. G. Lee, S. M. Woo, S. U. Seo, C. H. Lee, M. C. Baek, S. H. Jang, Z. Y. Park, S. Yook, J. O. Nam and T. K. Kwon, *Exp. Mol. Med.*, 2024, **56**, 383–394.
6 F. Sun, H. Li, D. Sun, S. Fu, L. Gu, X. Shao, Q. Wang, X. Dong, B. Duan, F. Xing, J. Wu, M. Xiao, F. Zhao, J. J. Han, Q. Liu, X. Fan, C. Li, C. Wang and T. Shi, *Sci. China Life Sci.*, 2025, **68**, 5–102.
7 M. L. Kovarik and N. L. Allbritton, *Trends Biotechnol.*, 2011, **29**, 222–230.
8 S. Sakamoto, T. Komatsu, R. Watanabe, Y. Zhang, T. Inoue, M. Kawaguchi, H. Nakagawa, T. Ueno, T. Okusaka, K. Honda, H. Noji and Y. Urano, *Sci. Adv.*, 2020, **6**, eaay0888.

9 J. Qin, X. Li, L. Cao, S. Du, W. Wang and S. Q. Yao, *J. Am. Chem. Soc.*, 2020, **142**, 417–423.
10 I. Joanito, P. Wirapati, N. Zhao, Z. Nawaz, G. Yeo, F. Lee, C. L. P. Eng, D. C. Macalinao, M. Kahraman, H. Srinivasan, V. Lakshmanan, S. Verbandt, P. Tsantoulis, N. Gunn, P. N. Venkatesh, Z. W. Poh, R. Nahar, H. L. J. Oh, J. M. Loo, S. Chia, L. F. Cheow, E. Cheruba, M. T. Wong, L. Kua, C. Chua, A. Nguyen, J. Golovan, A. Gan, W. J. Lim, Y. A. Guo, C. K. Yap, B. Tay, Y. Hong, D. Q. Chong, A. Y. Chok, W. Y. Park, S. Han, M. H. Chang, I. Seow-En, C. Fu, R. Mathew, E. L. Toh, L. Z. Hong, A. J. Skanderup, R. DasGupta, C. J. Ong, K. H. Lim, E. K. W. Tan, S. L. Koo, W. Q. Leow, S. Tejpar, S. Prabhakar and I. B. Tan, *Nat. Genet.*, 2022, **54**, 963–975.
11 J. G. Keller, M. Stougaard and B. R. Knudsen, *Methods Enzymol.*, 2019, **628**, 43–57.
12 N. S. Punekar, *Isotope Effects in Enzymology*, Springer, Singapore, 2025.
13 G. Li, J. E. Montgomery, M. A. Eckert, J. W. Chang, S. M. Tienda, E. Lengyel and R. E. Moellering, *Nat. Commun.*, 2017, **8**, 1775.
14 R. M. Phillips, E. Bair, D. S. Lawrence, C. E. Sims and N. L. Allbritton, *Anal. Chem.*, 2013, **85**, 6136–6142.
15 C. A. Proenca, T. A. Baldo, T. A. Freitas, E. M. Materon, A. Wong, A. A. Duran, M. E. Melendez, G. Zambrano and R. C. Faria, *Anal. Chim. Acta*, 2019, **1071**, 59–69.
16 J. Zhu, Y. Bai, X. Chen, L. Hu, W. Zhang, C. Liu, H. Shao, J. Sun and Y. Chen, *Chem. Sci.*, 2022, **13**, 12799–12807.
17 X. Shi, B. Xi, P. Jasbi, C. Turner, Y. Jin and H. Gu, *Anal. Chem.*, 2020, **92**, 11728–11738.
18 I. Schechter and E. Ziv, *Biol. Chem.*, 2008, **389**, 313–320.
19 A. Lechner, P. Wolff, E. Leize-Wagner and Y. N. Francois, *Anal. Chem.*, 2020, **92**, 7363–7370.
20 M. Yao, Y. Wang, L. Cornwell, C. E. Sims and N. L. Allbritton, *Anal. Chem.*, 2025, **97**, 2981–2990.
21 Y. Han, C. Qiu, F. Gao, K. Cao, P. Cao, Y. Tang, Y. Duan, H. Zou, H. Yuan, X. Gao and L. Gao, *ACS Nano*, 2025, **19**, 20765–20778.
22 J. Hu, F. Liu, N. Feng and H. Ju, *Anal. Chim. Acta*, 2019, **1064**, 1–10.
23 P. M. Doran, *Homogeneous Reactions*, Academic Press, 2013.
24 K. A. Johnson and T. L. Dangerfield, *Design and interpretation of experiments to establish enzyme pathway and define the role of conformational changes in enzyme specificity*, Academic Press, 2023.
25 Z. Deng, J. Mao, Y. Wang, H. Zou and M. Ye, *Mol. Cell. Proteomics*, 2017, **16**, 135–145.
26 H. Ooka, Y. Chiba and R. Nakamura, *Nat. Commun.*, 2023, **14**, 4860.
27 Y. Xu, X. Liu, M. A. Ahmad, Q. Ao, Y. Yu, D. Shao and T. Yu, *Mater. Today Bio*, 2024, **27**, 101125.
28 E. Boedtkjer and S. F. Pedersen, *Annu. Rev. Physiol.*, 2020, **82**, 103–126.
29 L. B. Alcaraz, A. Mallavialle, T. David, D. Derocq, F. Delolme, C. Dieryckx, C. Mollevi, F. Boissiere-Michot, J. Simony-Lafontaine, S. Du Manoir, P. F. Huesgen, C. M. Overall, S. Tartare-Deckert, W. Jacot, T. Chardes, S. Guiu, P. Roger, T. Reinheckel, C. Moali and E. Liaudet-Coopman, *Theranostics*, 2021, **11**, 6173–6192.
30 M. A. Bewley, T. K. Pham, H. M. Marriott, J. Noirel, H. P. Chu, S. Y. Ow, A. G. Ryazanov, R. C. Read, M. K. Whyte, B. Chain, P. C. Wright and D. H. Dockrell, *Mol. Cell. Proteomics*, 2011, **10**, 008193.
31 W. Zhang, F. Xu, J. Yao, C. Mao, M. Zhu, M. Qian, J. Hu, H. Zhong, J. Zhou, X. Shi and Y. Chen, *Nat. Commun.*, 2023, **14**, 2485.
32 S. J. Altschuler and L. F. Wu, *Cell*, 2010, **141**, 559–563.
33 J. Lan, G. Wei, J. Liu, F. Yang, R. Sun and H. Lu, *Theranostics*, 2022, **12**, 2598–2612.
34 Y. Tie, H. Zheng, Z. He, J. Yang, B. Shao, L. Liu, M. Luo, X. Yuan, Y. Liu, X. Zhang, H. Li, M. Wu and X. Wei, *Signal Transduct. Targeted Ther.*, 2020, **5**, 6.
35 A. N. Anderson, P. Conley, C. D. Klocke, S. K. Sengupta, A. Pang, H. C. Farley, A. R. Gillingham, A. D. Dawson, Y. Fan, J. A. Jones, S. L. Gibbs, A. H. Skalet, G. Wu and M. H. Wong, *Biomark. Res.*, 2024, **12**, 67.
36 T. T. Aye, T. Y. Low, Y. Bjorlykke, H. Barsnes, A. J. Heck and F. S. Berven, *Anal. Chem.*, 2012, **84**, 4999–5006.
37 D. Bastida-Ruiz, K. Van Hoesen and M. Cohen, *Int. J. Mol. Sci.*, 2016, **17**, 638.
38 P. Siuti, S. T. Retterer, C. K. Choi and M. J. Doktycz, *Anal. Chem.*, 2012, **84**, 1092–1097.